BioOne DIGITAL LIBRARY

Event-Based Stable Isotope Analysis of Precipitation Along a High Resolution Transect on the South Face of O‘ahu, Hawai‘i

Authors: Booth, Honour, Lautze, Nicole, Tachera, Diamond, and Dores, Daniel

Source: Pacific Science, 75(3) : 421-441

Published By: University of Hawai'i Press

URL: https://doi.org/10.2984/75.3.9

The BioOne Digital Library (https://bioone.org/) provides worldwide distribution for more than 580 journals and eBooks from BioOne’s community of over 150 nonprofit societies, research institutions, and university presses in the biological, ecological, and environmental sciences. The BioOne Digital Library encompasses the flagship aggregation BioOne Complete (https://bioone.org/subscribe), the BioOne Complete Archive (https://bioone.org/archive), and the BioOne eBooks program offerings ESA eBook Collection (https://bioone.org/esa-ebooks) and CSIRO Publishing BioSelect Collection (https://bioone.org/csiro-ebooks).

Your use of this PDF, the BioOne Digital Library, and all posted and associated content indicates your acceptance of BioOne’s Terms of Use, available at www.bioone.org/terms-of-use.

Usage of BioOne Digital Library content is strictly limited to personal, educational, and non-commmercial use. Commercial inquiries or rights and permissions requests should be directed to the individual publisher as copyright holder.

BioOne is an innovative nonprofit that sees sustainable scholarly publishing as an inherently collaborative enterprise connecting authors, nonprofit publishers, academic institutions, research libraries, and research funders in the common goal of maximizing access to critical research.

Downloaded From: https://complete.bioone.org/journals/Pacific-Science on 05 Jul 2025
Terms of Use: https://complete.bioone.org/terms-of-use

Event-Based Stable Isotope Analysis of Precipitation Along a High Resolution Transect on the South Face of O'ahu, Hawai'i[1]

Honour Booth,[2,4] *Nicole Lautze*,[3] *Diamond Tachera*,[3] *and Daniel Dores*[3]

Abstract: While the influence of elevation and seasonal variation on isotopic composition has been studied on Maui, Hawai'i Island, and O'ahu (Scholl et al. 1996, Scholl et al. 2002, Scholl et al. 2007, Dores et al. 2020, Fackrell et al. 2020, Tachera et al. 2021), this work is the first to investigate event-based precipitation in detail on the island of O'ahu. The stable isotopic composition of water has been used to track the movement of water within the hydrosphere, to investigate the type and origin of a rainfall event, and elevation of collection, among other characteristics. Here, we present a high-resolution study of the stable isotopes δ^2H and $\delta^{18}O$ of precipitation along a compact land-to-sea transect in Waikīkī, a southwest facing region on O'ahu. The study provides a unique, in-depth investigation into the nature of individual storm events, and how they contribute to a larger seasonal climatic pattern. Monthly precipitation samples were collected at three sites along the transect from December 2017 to March 2019 and event-based samples were collected at the Makai site from October 2018 to February 2019. Storm direction, temperature, and relative humidity were recorded for each event-based sample. Results suggest that evaporative conditions at different elevations influence the isotopic composition of precipitation, either through net addition as moisture recycling, or net loss of evaporated water. The spatial distribution of these patterns from site to site illustrates the extreme heterogeneity of Hawaiian watersheds.

Keywords: stable istopes, precipitation, deuterium excess, tropical climate, hydrology

FOR TROPICAL ISLANDS, where precipitation becomes the groundwater resource used for drinking water, investigating the origin of recharge as precipitation is important for understanding the relationship between groundwater and its source. The stable isotopic composition of water ($\delta^{18}O$ and δ^2H) has been used to track the movement of water within the hydrosphere, helping to investigate the type and origin of a rainfall event, direction it traveled, and elevation at which the precipitation was collected, among other characteristics. The value of these isotopic ratios in precipitation are dependent on many hydrologic and climatic factors, such as source composition, relative humidity (RH) at the time of precipitation, and other evaporative conditions.

Worldwide, the linear relationship between $\delta^{18}O$ and δ^2H is explained with the global meteoric water line (GMWL), reflecting climatic processes on a global scale (Craig 1961). Due to the unique and diverse microclimates of tropical islands, recording

[1]Manuscript accepted 17 May 2021.
[2]University of Hawai'i at Mānoa, Department of Chemistry, HI, USA.
[3]University of Hawai'i at Mānoa, Hawai'i Institute of Geophysics and Planetology, HI, USA.
[4]Corresponding author (e-mail: honour@hawaii.edu).

Pacific Science (2021), vol. 75, no. 3:421–441
doi:10.2984/75.3.9

This work is licensed under a Creative Commons Attribution-NonCommercial-NoDerivatives 4.0 International License.

Downloaded From: https://complete.bioone.org/journals/Pacific-Science on 05 Jul 2025
Terms of Use: https://complete.bioone.org/terms-of-use

stable isotope values in regional precipitation is necessary to create local meteoric water lines (LMWLs). The LMWL then becomes a useful tool in defining the relationship between $\delta^{18}O$ and $\delta^{2}H$ in the local precipitation recharging the groundwater of the island, and can help determine important climatic processes defining rainfall events (Putman et al. 2019). Deviations from the LMWL are caused by the evaporative conditions that control the isotopic fractionation of water, as the lighter isotopes, ^{16}O and ^{1}H, preferentially go into the vapor phase while the heavier isotopes, ^{18}O and ^{2}H, remain in the liquid phase (Dansgaard 1964, Kendall and Caldwell 1998). The resulting $\delta^{18}O$ (‰) and $\delta^{2}H$ (‰) values can be explained by the amount effect, the observed phenomena where greater precipitation depths result in more negative $\delta^{18}O$ and $\delta^{2}H$ values, and deuterium excess (*d*), defined as

$$d(\%) = \delta^{2}H - 8\delta^{18}O \quad (1)$$

and mathematically related to the *y*-intercept of the GMWL (Dansgaard 1964). Amount effect and *d* are often used to investigate past climate and weather, as their influence on the meteoric water line can describe moisture source, seasonal influence, and conditions during evaporation and precipitation (Lee and Fung 2006, Pfahl and Sodemann 2012, Winnick et al. 2014, Tharammal et al. 2017). RH controls whether evaporate accumulates on the precipitate or the precipitate evaporates. High temperatures and high RH cause the evaporation of land-based moisture sources, while high temperatures and low RH cause evaporation of the falling precipitation.

While the influence of elevation and seasonal variation on isotopic composition has been studied on Maui, Hawai'i Island, and O'ahu (Scholl et al. 1996, Scholl et al. 2002, Scholl et al. 2007, Dores et al. 2020, Fackrell et al. 2020), this work is the first to investigate event-based precipitation in detail, with a focus on the island of O'ahu. Previous studies in the tropics had success in rainfall characterization (Munksgaard et al. 2019) and differentiating the event type of precipitation, such as orographic rainfall vs. low-pressure systems (Scholl et al. 2009, Zwart et al. 2018). While stable isotope studies on the hydrological cycle within Hawai'i have focused on precipitation over long sampling intervals and large geographical areas, there is a need for stable isotope data at higher spatial and temporal resolutions in order to further define the characteristics of individual precipitation events and how they relate to groundwater recharge. Recent studies highlight the need for both the long-term monitoring of the isotopic composition of precipitation in Hawai'i (Tachera et al. 2021) and finer resolution sampling to better understand the importance of event-based precipitation (Dores et al. 2020). Here, we focus on the latter, with an experimental design to improve the spatial and temporal resolution of precipitation collection studies. Our high-resolution study occurs along a compact land to sea transect in the highly urbanized Waikīkī ahupua'a (land division), a Kona (southwest) facing region on the island of O'ahu (Figure 1). We use $\delta^{18}O$, $\delta^{2}H$, and *d* values and storm track data to establish how individual precipitation events contribute to the isotopic composition of the monthly and seasonal precipitation samples. We hypothesize that while trade wind storms are responsible for most of the precipitation experienced along the transect, offshore and Kona storms contributed greatly to rainfall, especially at the lowest elevation site.

BACKGROUND

The sampling transect is located in the ahupua'a of Waikīkī in the Kona moku (district) of O'ahu (Figure 1). Characteristic of ahupua'a within a Kona moku, Waikīkī is relatively dry compared to trade wind facing locations, receiving an average of 600 mm of rainfall annually (Chu et al. 2010, Giambelluca et al. 2013). Precipitation in Waikīkī is predominantly the result of residual orographic and onshore rainfall, either from local offshore evaporation or Kona storm events. The intensity of these different types of rainfall varies from year to year due to large climatic patterns in the Pacific.

Downloaded From: https://complete.bioone.org/journals/Pacific-Science on 05 Jul 2025
Terms of Use: https://complete.bioone.org/terms-of-use

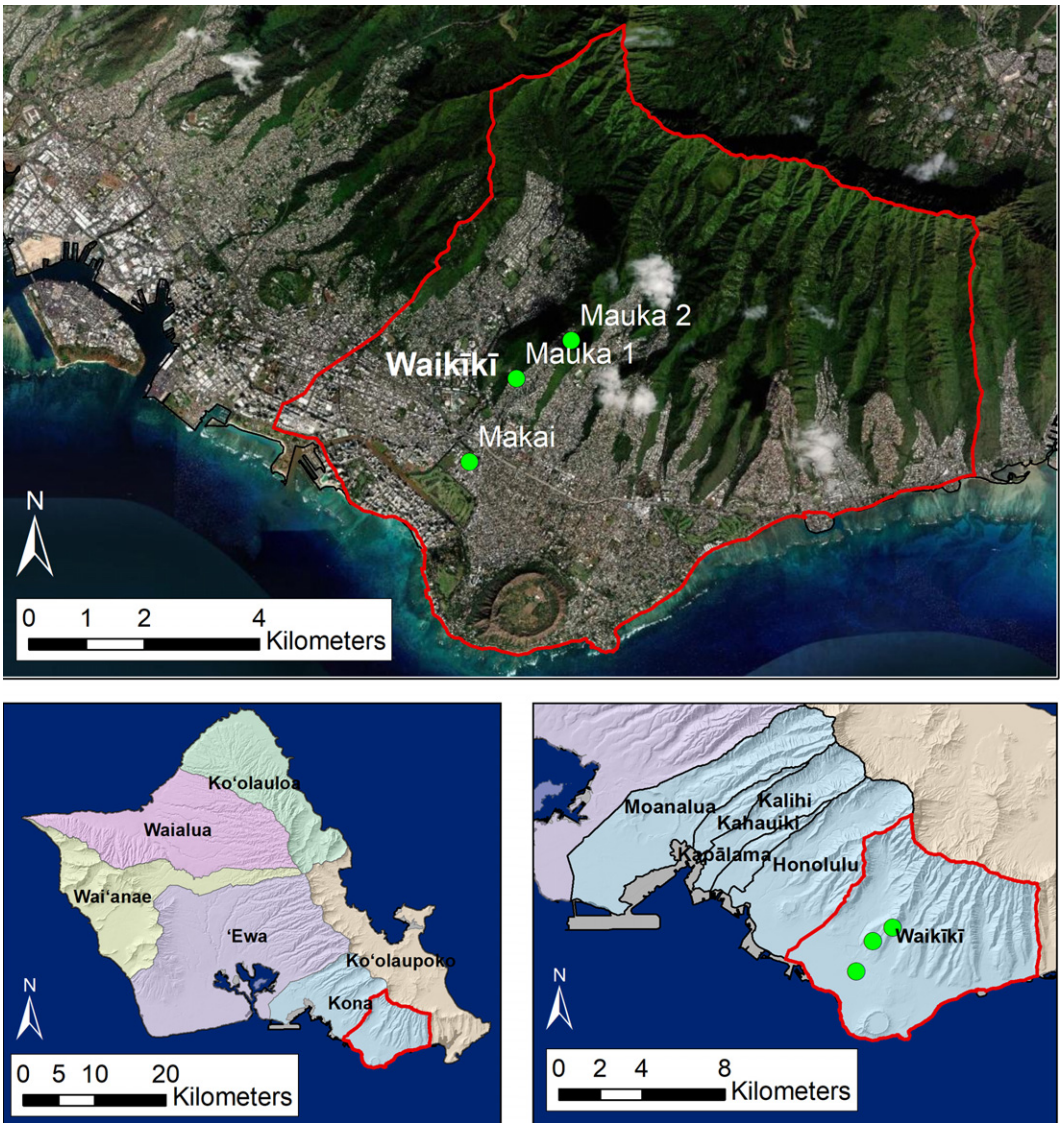

FIGURE 1. Map of sampling transect within the Waikīkī ahupua‘a in the Kona moku of O‘ahu.

Seasonal Weather Patterns on O‘ahu

The Hawaiian Islands experience two main seasons: Ho‘oilo, the wet season, and Kauwela, or Kau, the dry season (NOAA 2018, 2019). The transition to Ho‘oilo begins in October and lasts until April. During Ho‘oilo, O‘ahu experiences consistent trade wind storms and occasional Kona storms of local or cyclonic origin and bouts of Kona wind. Daily Ho‘oilo weather generally has cooler temperatures and higher humidity. Kau extends from May until October; trade winds dominate this season while Kona winds are extremely rare. Rainfall is less frequent in Kau, especially in Kona districts, with brief periods of diminished trade winds. Hurricane season begins in Kau and extends into Ho‘oilo, typically lasting from June to November (OPHP 2020).

Downloaded From: https://complete.bioone.org/journals/Pacific-Science on 05 Jul 2025
Terms of Use: https://complete.bioone.org/terms-of-use

The seasons and climate of O'ahu and the other Hawaiian Islands are influenced by both El Niño Southern Oscillation (ENSO) and Pacific Decadal Oscillation (PDO). Interactions between ENSO and PDO can cause variability in seasonal rainfall, resulting in uncharacteristic conditions during the typical wet and dry seasons (Chu and Chen 2005). Climate change has been shown to exacerbate out of season conditions and is broadly thought to cause a decline in rainfall (Chu et al. 2010, Diaz et al. 2011).

Deuterium Excess

Froehlich et al. (2002) portrayed d relative to the GMWL as a gradient deviating away from the GMWL in both directions. The d gradient above the GMWL ($d > 10$) is representative of precipitation that has experienced enhanced moisture recycling, when evaporation from local moisture sources accumulates onto falling precipitate. Through isotopic fractionation, ^{16}O and ^{1}H preferentially go into the vapor phase, making the accumulating evaporate rich in ^{16}O and ^{1}H (Dansgaard 1964, Kendall and Caldwell 1998). The result is an increase in d and more negative $\delta^{18}O$ and $\delta^{2}H$ values of the precipitation sample. The d gradient below the GMWL ($d < 10$) is representative of precipitation that has experienced loss due to evaporation, when falling precipitate evaporates as it descends. Through isotopic fractionation, ^{16}O and ^{1}H preferentially evaporate, leaving behind the heavier isotopes, ^{18}O and ^{2}H, as the liquid phase precipitate (Dansgaard 1964, Kendall and Caldwell 1998). The result is a decrease in d and less negative $\delta^{18}O$ and $\delta^{2}H$ values of the precipitation sample.

METHODS

A precipitation sample from each of the three sites was collected monthly from December 2017 to March 2019. Additionally, a total of 38 event-based samples were collected at the Makai site from October 2018 to February 2019. Data related to the following variables were collected for each sample: stable isotopes $\delta^{18}O$ and $\delta^{2}H$, volume, elevation, temperature, RH, and storm direction.

Collector Assembly and Deployment

Two types of precipitation collectors were constructed following the methodologies of Scholl et al. (1996): (1) those intended for long-term deployment and monthly collection frequency, and (2) those deployed to collect individual storm or rain events. Monthly precipitation collectors were built using food grade HDPE 5 gal buckets, 9-cm diameter Buchner funnels, and silicone caulking. Buchner funnels were set in the bucket lids and sealed using a rubber grommet and silicon caulking. At each collection site, the collectors were positioned so as to maximize exposure to the sky during precipitation events, and fastened to fencing using bungee cords for stability against storm conditions. Approximately 500 mL of mineral oil was added to each collector to prevent evaporation of collected rainfall. All monthly precipitation collectors were deployed at the respective sites on 28 November 2017 (Figure 1). Individual storm sample collectors consisted of a Buchner funnel placed in a collection bottle fastened to fencing adjacent to the monthly precipitation collector at the Makai site. No mineral oil was added to the collection bottle as samples were collected as soon as possible, and some cases immediately, following each storm event to minimize the effects of evaporation.

Sample Collection and Preparation

Over the 16-month sampling period, samples from each site were typically collected over one-month intervals from December 2017 to March 2019, resulting in a total of 12 samples from each site. As the Makai site experienced very little rain during the summer months of 2018, only one sample was collected from May to August. Mauka 1 and Mauka 2 samples from May to August were analyzed individually; the VWA was calculated for these samples so comparisons could be made along

Downloaded From: https://complete.bioone.org/journals/Pacific-Science on 05 Jul 2025
Terms of Use: https://complete.bioone.org/terms-of-use

the transect. Due to logistical reasons, one sample was collected from each site for the months of December 2018 and January 2019.

Samples were filtered using standard bleached paper filters on site, followed by Whatman Grade 1 paper filters in the laboratory until all mineral oil was removed. Mineral oil filtered on site was returned to the precipitation collector after separation. Samples were stored in either 500 mL amber glass bottles or 250 mL HPDE bottles and refrigerated until the time of analysis. To homogenize the water before subsampling, sample bottles were shaken before 2 mL aliquots were transferred to a 2 mL glass vial. To prevent evaporation, vial caps were wrapped with Parafilm. Samples were arranged from expected lowest $\delta^{18}O$ (‰) value to expected highest $\delta^{18}O$ (‰) value and refrigerated until analysis. Volumes of all samples were measured during sample preparation.

Event-based precipitation samples were collected daily from October 2018 through February 2019. Of the total 38 samples collected, 11 samples are representative of single rainfall events, 7 of which are from prolonged rain events lasting over an hour. A precipitation event was considered "single" if the precipitation rate did not go to zero. Events during which the precipitation rate was recorded by the Kaimukī High School station (KHIHONOL118) on Weather Underground to reach zero for any duration during the course of an event are then considered as "multiple-shower" events.

Sample Analysis

$\delta^{18}O$ and $\delta^{2}H$ values of water were determined using an L2130-*i* Picarro cavity ring down spectrometer fitted with an A0211 High Precision Vaporizer and HTC PAL autosampler at the School of Ocean and Earth Science and Technology's Biogeochemical Stable Isotope Facility at the University of Hawai'i at Mānoa. Water aliquots (1.8 μL) were evaporated and equilibrated with clean-dry nitrogen (N_2) gas. Measured isotope values were normalized to VSMOW using three laboratory reference materials: KONA desalinated deep seawater (0.51‰ for $\delta^{18}O$ and 1.54‰ for $\delta^{2}H$), LAB DI laboratory deionized water (−5.11‰ for $\delta^{18}O$ and −20.43‰ for $\delta^{2}H$), and MKSNOW melted snow collected from the Mauna Kea summit (−13.44‰ for $\delta^{18}O$ and −96.81‰ for $\delta^{2}H$). Laboratory references were extensively calibrated with NIST reference materials that bracket the $\delta^{2}H$ and $\delta^{18}O$ values of the in-house standards, including Reference standards Standard Light Antarctic Precipitation-2 (SLAP-2), Vienna Standard Mean Ocean Water - 20 (VSMOW-2), and Greenland Ice Sheet Precipitation (GISP) from the International Atomic Energy Agency (Vienna, Austria), and by inter-laboratory comparison. These in-house standards were analyzed between every 10–14 unknown samples, along with a check sample (Evian bottled water, also extensively characterized using the above-mentioned isotope reference materials). Analytical uncertainty was determined by taking the average of at least triplicate sample injections and calculating the standard deviation from the average for each sample. Samples were analyzed in the order of expected isotopic composition and the first three injections of each sample were ignored to minimize memory carry-over effects. The isotope analysis results were post-processed using Picarro "Chemcorrect" software to flag for organic contamination. Any samples that were flagged for such contamination are not reported.

Data Preparation and Analysis

Wind and storm direction were determined from weather station data on Weather Underground and base reflectivity doppler radar archives from weather.us, respectively. Times of precipitation were identified with rain gauge data from the Kaimukī High School weather station, and wind direction was recorded. The identified times were then used to watch the appropriate storms in the base reflectivity doppler radar archives for O'ahu. Storm track and direction were recorded for the precipitation times, and dominant storm direction was determined

Downloaded From: https://complete.bioone.org/journals/Pacific-Science on 05 Jul 2025
Terms of Use: https://complete.bioone.org/terms-of-use

based on sample volume and frequency of direction. While storm direction was highly variable, for the purpose of this study, general storm track and direction classified as "Northerly" or "Southerly" was sufficient. Storm track direction associated with larger collected sample volumes were weighted higher in determining a dominant storm direction.

The yearly volume-weighted average (VWA) of $\delta^{18}O$ and $\delta^{2}H$ was calculated from monthly samples for each site to establish both variation in time across the transect and variation in time throughout the year. When certain sites could not be collected at a monthly resolution, a multi-month VWA of $\delta^{18}O$ and $\delta^{2}H$ for the other sites was calculated for that time interval to provide comparable results. The $\delta^{18}O$ and $\delta^{2}H$ values of individual storm samples were also used to calculate a monthly VWA for comparison against monthly $\delta^{18}O$ and $\delta^{2}H$ values. This comparison serves as a first order investigation into how event-based samples aggregate into precipitation on a monthly scale. A linear regression was applied to the stable isotope values to calculate a LMWL for the transect in terms of monthly and event-based precipitation. The LMWL is an efficient tool to compare the results of this study to other precipitation collection efforts across the Hawaiian Islands. Deuterium-excess was calculated for each sample to determine variability across events and from site to site, with a specific focus on evaporative processes and moisture recycling.

RESULTS

Weather During the Sampling Period

The sampling period occurred over a 16-month period spanning two consecutive Hoʻoilo, during a transition from La Niña to El Niño conditions while in a high rainfall epoch of Pacific Decadal Oscillation (Chu and Chen 2005, NOAA 2018, 2019). Monthly precipitation collectors were deployed on 28 November 2017, in the middle of the 2017–2018 Hoʻoilo (NOAA 2018). Weak La Niña influences resulted in wet conditions that were experienced on the leeward faces of Oʻahu for the duration of the season. In congruence with rainfall throughout Hawaiʻi, the sampling transect on Oʻahu experienced drier conditions in January with heavy rains from February to April. Unique to the transect, our sampling stations received more rain in December than the surrounding regions of Hawaiʻi.

The 2018 Kau was considered to be the second wettest in the last 30 years. Some leeward areas on Oʻahu were subject to drought. Lower elevation areas within the transect experienced light rainfall from May to August. However, higher elevations in the transect experienced higher rainfall, as residue from storms on the windward side of the Koʻolau range. A majority of the precipitation during Kau occurred at the end of the season in August and September.

The 2018–2019 Hoʻoilo was influenced by weak El Niño conditions, with drought developing at lower elevations on the leeward faces of the islands (NOAA 2019). The sampling transect typically experienced rainfall similar to that of the general geography. The sampling period ended one month before the end of the wet season. Oʻahu was the only Hawaiian Island that did not develop drought due to dry periods during January and March of 2019.

Two major storm events occurred during the sampling period. The first was a flash flood event from 13–15 April 2018. On April 13th, the southern Koʻolau mountain range on Oʻahu experienced precipitation rates of over 4 inches per hour from 7:00 pm to 9:00 pm HST (NWS 2018). The event was highly localized and only affected windward communities from Maunawili to Waimānalo and leeward communities from Hawaiʻi Kai to Mānoa. The storm intensified to the west, and severely impacted Kauaʻi over the next two days. The second major storm event was Hurricane Lane, which entered the Central Pacific on 18 August 2018 and departed from the main Hawaiian Islands on 26 August 2018 (Beven and Wroe 2019). While Lane did not make landfall, the main Hawaiian Islands did experience high winds and heavy rains. Hawaiʻi Island, Maui, and the windward side of Oʻahu were most heavily impacted. Within

Downloaded From: https://complete.bioone.org/journals/Pacific-Science on 05 Jul 2025
Terms of Use: https://complete.bioone.org/terms-of-use

the sampling transect, both Mauka sites experienced rainfall, although no rainfall occurred at the Makai site.

Event-Based Samples

Twenty-four of the samples came from storms originating in the North, and 14 of the samples came from storms originating in the South. The isotopic composition of the event-based samples were highly variable, ranging from -6.9 ± 0.04‰ $\delta^{18}O$ and -49.9 ± 0.25‰ $\delta^{2}H$ in February 2019 to -2.7 ± 0.06‰ $\delta^{18}O$ and 19.0 ± 0.19‰ $\delta^{2}H$ in November 2018 (Table 1). Both of these months had rainfall events predominantly from the Northeast, although 3 storms in February originated in the SW. The individual storm with the greatest rainfall depth during the sampling period was from a SSE-originating storm in October 2018, at 33 mm. The average individual storm rainfall depth was 5 mm.

To determine validity of individual storm samples, monthly $\delta^{18}O$, $\delta^{2}H$, and *d* data from October 2018 to February 2019 were compared with the VWAs of individual rain samples for each respective month (Table 2). Where VWAs for monthly and individual rain samples did not agree, the lag time between the end of the rain event and collection of the sample was considered (Table 1). As there was no apparent correlation between lag times and agreement of VWAs for monthly and individual samples, evaporation of individual samples was considered negligible.

Monthly Samples

The volume-weighted average $\delta^{18}O$ and $\delta^{2}H$ values were −2.69‰ and −12.89‰, −2.76‰ and −11.60‰, and −2.98‰ and −11.65‰ for the Makai, Mauka 1, and Mauka 2 sites, respectively. The isotopic composition of precipitation along the transect ranged from -4.76 ± 0.07‰ $\delta^{18}O$ and -27.53 ± 0.20‰ $\delta^{2}H$ from September 2018 to -0.20 ± 0.02‰ $\delta^{18}O$ and 5.70 ± 0.18‰ $\delta^{2}H$ from January 2018, with the lightest value from the Mauka 2 site and the heaviest value from the Makai site (Table 3). Most rainfall events in September 2018 came from the East-Northeast direction, with only one, two-day event originating in the South (Table 4). Rainfall events in January 2018 were infrequent and came predominantly from the Southeast and Southwest directions (Table 4).

The average rainfall depths for the Makai, Mauka 1, and Mauka 2 sites were 65 mm, 66 mm, and 92 mm, respectively. The Mauka 2 site samples frequently had the highest rainfall depth per sampling interval, ranging from 19 mm in January 2018 to 145 mm in October 2018 for a single month (Table 3). The only exception to this was for March 2018 and February 2019, when monthly samples from the Makai site were 99 mm and 142 mm, respectively (Table 3). The months of January 2018 and March 2019 had the lowest rainfall depths along the transect (Table 3). The LMWL ($\delta^{2}H = 6.87\delta^{18}O + 7.02$) for the sampling transect was calculated using linear regression analysis of $\delta^{18}O$ and $\delta^{2}H$ values of individual monthly samples from each site (Figure 2).

DISCUSSION

The isotopic composition of precipitation is influenced by multiple factors, including distance from the origin of the source of moisture, elevation of the collection site, and evaporative processes driven by temperature and RH. The influence of elevation and seasonal variation on evaporative conditions, and the resulting isotopic composition of precipitation, are discussed below.

Event-Based Precipitation

Event-based precipitation samples show how the evaporative conditions at low elevation produce various types of precipitation, as well as how individual precipitation events contribute to monthly precipitation. The Makai site regularly had a rainfall depth greater than or equal to the Mauka sites, which typically experience conditions more conducive to heavy precipitation events (Table 1). Generally, convective storms such as Kona Lows

Downloaded From: https://complete.bioone.org/journals/Pacific-Science on 05 Jul 2025
Terms of Use: https://complete.bioone.org/terms-of-use

TABLE 1

Isotopic Composition, Volume, and Weather Conditions for Event-Based Samples Collected at the Makai Site

Sample Number	Sampling Date	Rainfall Depth (mm)	$\delta^{18}O$ (‰)	$\delta^{2}H$ (‰)	*d* (‰)	*T* (° F)	RH (%)	Wind Direction	Storm Direction	Collection Lag Time (min)
1	10/19/2018	0.5	−0.5	2.5	6.5	81.2	90.6	ENE	ENE/S	540
2	10/23/2018	0.9	0.3	7.7	5.3	80.6	84.4	NE	NE	615
3	10/26/2018	1.4	2.3	16.4	−2	82.0	90.8	NE	SSE	515
4	10/27/2018	0.4	−0.2	4.5	6.1	81.3	86.9	NE	ESE	405
5	10/30/2018*	8.8	−5.1	−27.2	13.6	86.4	92.1	SSE	ESE	50
6	10/30/2018	23.4	−5.0	−26.1	13.9	86.4	92.1	SSE	ESE	50
7	10/30/2018	33.2	−3.5	−14.7	13.3	86.9	96.9	SSE	SSE	535
8	10/31/2018	0.6	−4.7	−27.3	10.3	no data	no data	NE	SSE	0
9	11/2/2018	1.7	−0.6	4	8.8	77.3	79.2	NE	ENE	45
10	11/16/2018	2.9	−0.7	3.6	9.2	78.1	84.5	NE/ENE	ENE	111
11	11/17/2018	0.7	2.7	19	−2.6	78.8	91.4	NE/ENE	ENE	431
12	11/26/2018	0.4	1.2	13.1	3.5	80.6	91.9	NE	NNE	136
13	12/6/2018	6.8	−2.0	−1.3	14.7	77.0	83.8	NE	SSE/NW	61
14	12/7/2018	4.6	−1.3	2.1	12.5	76.7	82.4	NE	ESE/ENE	11
15	12/8/2018	5.3	−0.6	9.2	14	77.2	87.7	ENE	NNE	1219
16	12/10/2018	2.5	−0.9	4.4	11.6	76.9	78.6	NE	ENE	114
17	12/18/2018	0.7	0.2	11.5	9.9	74.8	79.9	E	ENE	576
18	12/28/2018	0.5	−1.5	−8.3	3.7	97.5	no data	ENE	SW	59
19	12/29/2018	4.9	−2.7	−14.6	7	83.3	95.1	ENE	SW	101
20	12/31/2018	0.3	0.1	7.1	6.3	77.2	81.2	ENE	ENE	46
21	1/25/2019	0.6	−0.4	5.7	8.9	80.3	91.4	SW	NW	141
22	1/30/2019	10.2	−1.1	−1.9	6.9	75.7	76.8	NNW	NNE	0
23	1/31/2019	14.5	−2.8	−15.3	7.1	75.8	83.9	NNE/ENE	NNE	26
24	2/1/2019	7.5	−2.3	−14.1	4.3	77.0	77.9	ENE/NE	NNE	941
25	2/6/2019	2.4	−3.1	−14.3	10.5	77.7	89.3	SSW	SW	0
26	2/7/2019	6.0	−3.4	−13.2	14	85.9	100.6	SSW	SW	631
27	2/10/2019	0.8	0.1	13.0	12.2	64.3	79.5	NW	NW	11
28	2/13/2019	8.2	−4.3	−18.4	16	84.4	90.0	NE	NE	181
29	2/13/2019	0.3	−2.0	−2.6	13.4	92.7	90.2	NE	NE	6
30	2/13/2019	9.9	−4.8	−18.6	19.8	74.8	79.7	NE	NE	181
31	2/13/2019*	9.7	−4.3	−16.5	17.9	74.8	79.7	NE	NE	16
32	2/14/2019	3.1	−2.3	−5.8	12.6	68.6	71.6	NE	NE	346
33	2/15/2019	1.9	−1.4	3.9	15.1	71.0	67.3	ENE	NE	86
34	2/16/2019	3.8	−0.3	6.4	8.8	76.7	77.4	ENE/NNE	NE	406
35	2/19/2019	3.0	−2.9	−17.7	5.5	80.7	83.0	ESE	SSW	451
36	2/19/2019	3.5	−6.9	−49.9	5.3	90.8	91.8	ESE	SSW	21
37	2/25/2019	0.3	−1.3	−0.5	9.9	81.4	87.8	NE	NE	0
38	2/26/2019	5.2	−1.8	2.0	16.4	85.9	89.4	NE	NE	90

tend to be associated with more intense rain that is depleted in heavy isotopes, while stratiform or orographic rains like trade wind rainfall consist of lighter, smaller drops, usually under drier atmospheric conditions. During most of the months that the Makai site collected a monthly rainfall depth greater than or equal to either or both of the Mauka sites,

Downloaded From: https://complete.bioone.org/journals/Pacific-Science on 05 Jul 2025
Terms of Use: https://complete.bioone.org/terms-of-use

TABLE 2

Comparison of Isotopic Values for Monthly Samples and VWA of Event-based Samples

Month	$\delta^{18}O$	$\delta^{2}H$	*d*
October 2018			
Monthly	−3.10	−13.80	11.00
Storm VWA	−4.00	−19.00	13.00
November 2018			
Monthly	−0.60	4.50	9.30
Storm VWA	−0.10	6.30	7.20
December 2018/January 2019			
Monthly	−2.6	−14.9	5.9
Storm VWA	−1.8	−4.7	9.5
February 2019			
Monthly	−3.7	−14.7	14.9
Storm VWA	−3.4	−13.8	13.4

local winds were predominantly from the ESE (Table 1). Precipitation events at the Makai site varied from light, misting rains that produced scarce samples of 2 mL or less that can be characterized as trade wind precipitation, to heavy downpours that lasted for hours and accumulated over 33 mm of water that imply a convective source such as a Kona storm. While there was no relationship between isotopic composition and rainfall depth or isotopic composition and RH (Figures 3 and 4), these observations agree with the hypothesis that storm-based precipitation is a major source of rainfall in the lower elevation coastal areas of Hawai'i.

To assess variation in rainfall depth as well as the $\delta^{2}H$ and $\delta^{18}O$ values among different rainfall types, we focus on evaporative and moisture cycling conditions. Calculation of *d* and recorded values of temperature and RH for each event-based sample, in comparison to monthly samples, helped control for the effects of evaporation and moisture recycling on collected rainfall for each sample (not shown). Based on these three variables, controlling factors on sample collection could be determined, and their resulting impacts on isotopic compositions accounted for. First verified at an event-based sample scale, these trends are further investigated at the seasonal ("Influence of Seasonal Variation" section) and spatial ("Influence of Elevation

TABLE 3

Isotopic Composition and Volumes of Monthly Samples from Each Collection Site

Month	Rainfall Depth (mm)			$\delta^{18}O$ (‰)			$\delta^{2}H$ (‰)			*d* (‰)		
	Makai	Mauka 1	Mauka 2	Makai	Mauka 1	Mauka 2	Makai	Mauka 1	Mauka 2	Makai	Mauka 1	Mauka 2
Dec 2017	115.2	104.4	130.2	−4.20	−3.97	−3.73	−20.9	−18.8	−17.2	12.7	13.0	12.6
Jan 2018	10.4	11.8	19.0	−0.20	−0.90	−1.20	5.20	2.30	1.80	6.8	9.5	11.4
Feb 2018	116.2	78.1	129.5	−2.35	−3.30	−3.90	−9.55	−14.5	−18.3	9.3	11.9	12.9
Mar 2018	98.7	75.1	77.3	−3.50	−4.10	−3.90	−18.0	−20.3	−17.5	10.0	12.5	13.7
Apr 2018	130.9	99.0	141.2	−0.58	−1.64	−2.15	−3.89	−7.21	−8.45	0.7	5.9	8.7
May–Aug 2018	89.1	114.1	224.5	−1.30	−1.35	−1.55	−3.10	−3.29	−2.76	7.3	7.5	9.7
Sep 2018	114.0	114.3	118.7	−4.10	−4.14	−4.76	−26.8	−24.8	−27.5	6.0	8.4	10.5
Oct 2018	41.5	115.8	145.1	−3.10	−3.10	−2.90	−13.8	−12.1	−9.80	11.0	12.7	13.4
Nov 2018	41.5	88.5	108.6	−0.60	−1.50	−1.90	4.50	1.20	0.00	9.3	13.2	15.2
Dec 2018–Jan 2019	68.2	86.5	115.4	−2.60	−1.60	−3.00	−14.9	−7.10	−13.4	5.9	5.7	10.6
Feb 2019	141.8	86.5	137.5	−3.70	−3.60	−4.10	−14.7	−15.2	−15.9	14.9	13.6	16.9
Mar 2019	5.2	22.9	30.5	−0.20	−0.40	−1.00	4.70	7.20	4.00	6.3	10.4	12.0
Average	*81.1*	*83.1*	*114.8*	*−2.69*[a]	*−2.76*[a]	*−2.98*[a]	*−12.89*[a]	*−11.60*[a]	*−11.65*[a]	*8.65*[b]	*10.32*[b]	*12.19*[b]

[a] Volume-weighted average reported.
[b] Calculated by inputting the respective VWA of $\delta^{18}O$ and $\delta^{2}H$ of each site into the equation $d = \delta^{2}H - 8\delta^{18}O$.

Downloaded From: https://complete.bioone.org/journals/Pacific-Science on 05 Jul 2025
Terms of Use: https://complete.bioone.org/terms-of-use

TABLE 4

Monthly Weather Conditions along the Transect

Month	Temperature (°F)		Relative Humidity (%)		Wind Direction	Storm Direction
	Makai	Mauka	Makai	Mauka		
Dec 2017	78.8	74.2	63.0	72.8	ESE	ENE
Jan 2018	76.1	74.2	63.6	72.8	E	SE/SW
Feb 2018	76.5	73.2	70.9	80.8	ESE	SSE
Mar 2018	75.8	72.8	68.0	77.9	ESE	ENE
Apr 2018	77.3	74.9	72.9	83.5	E	ENE
May–Aug 2018	80.3	78.7	64.9	76.7	ENE*	ENE
Sep 2018	84.9	80.0	68.9	80.8	ENE	ENE
Oct 2018	83.4	78.9	68.9	82.8	ENE	ESE
Nov 2018	79.3	76.7	70.1	82.2	ENE	ENE
Dec 2018–Jan 2019	77.2	74.0	64.4	78.3	ENE/ESE	NNE
Feb 2019	76.9	70.5	58.3	80.9	ESE	NE
Mar 2019	74.9	72.7	55.3	75.2	E	NE

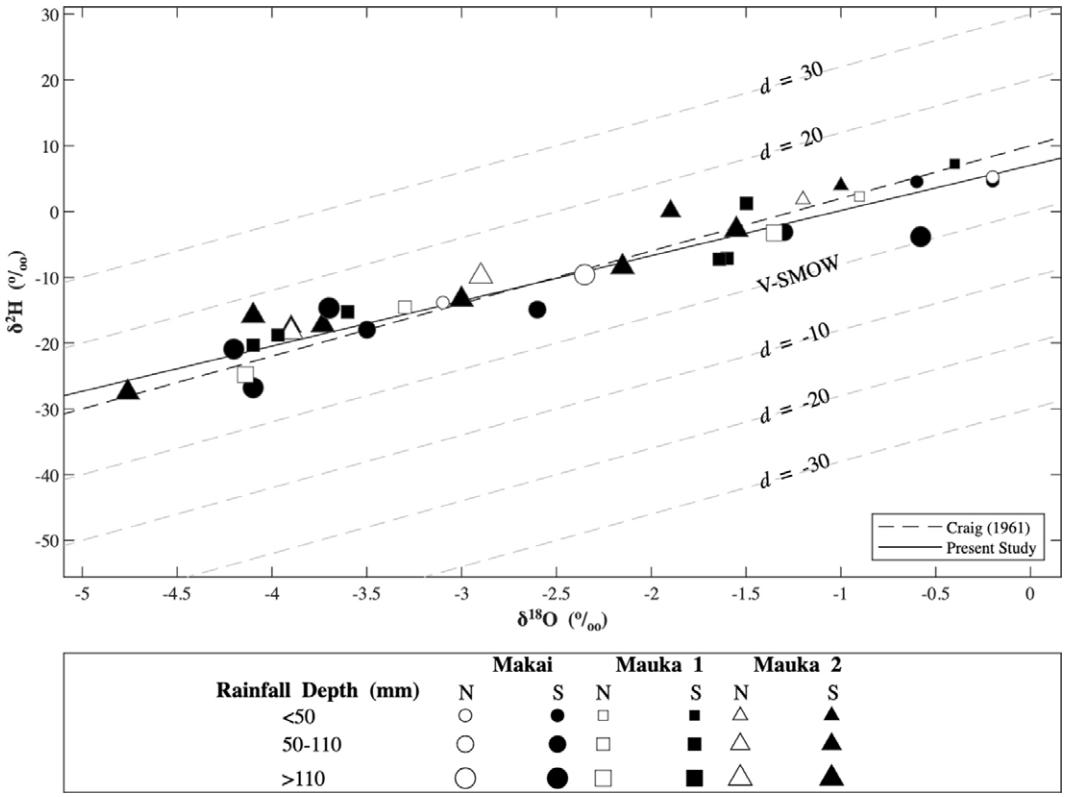

FIGURE 2. The local meteoric water line (LMWL), $\delta^2H = 6.87\delta^{18}O + 7.02$, produced with monthly samples, compared with the global meteoric water line (GMWL) from Craig (1961) and *d* gradients from Dansgaard (1964) and Froehlich et al. (2002).

Downloaded From: https://complete.bioone.org/journals/Pacific-Science on 05 Jul 2025
Terms of Use: https://complete.bioone.org/terms-of-use

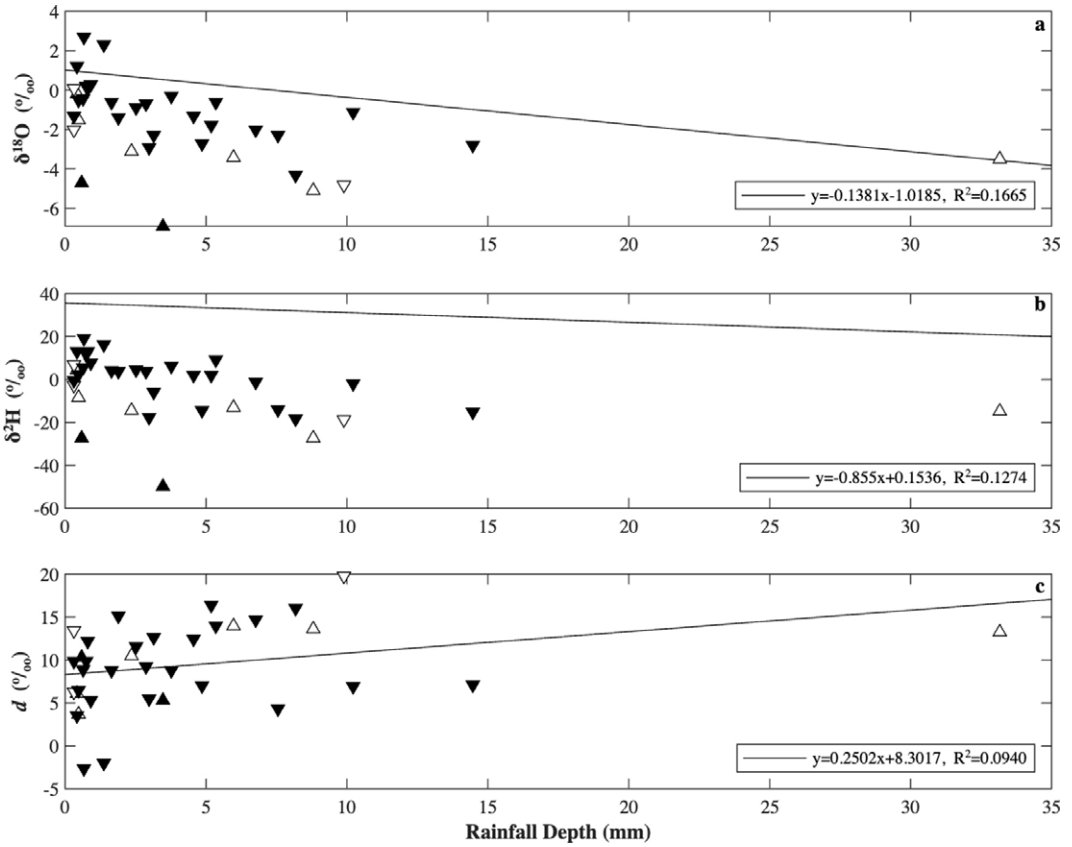

FIGURE 3. Linear regression of (*A*) $\delta^{18}O$, (*B*) $\delta^{2}H$, and (*C*) *d* values, from event-based precipitation, against corresponding rainfall depth. There is no relationship between rainfall depth and any of the stable isotope variables.

and Distance from Marine Moisture Source" section) scales.

Influence of Seasonal Variation

Most of the monthly rainfall depths from precipitation collectors aligned with monthly annual average rainfall depths for the nearest Rainfall Atlas station at UH Mānoa (Giambelluca et al. 2013). While there are some discrepancies across months from both Kau and Ho'oilo, these can be attributed to (1) the position of our experimental network versus the Rainfall Atlas site and (2) the seasonal variation discussed in "Weather During the Sampling Period" section. The Rainfall Atlas site corresponds to a location sampled by Dores et al. (2020)—a comparison of data from our sites with this site, which emphasized the influences of microclimates and regional geography, is at the bottom of this section.

The isotopic composition of precipitation along the transect varies based on the evaporative conditions at the different sites as they are subject to seasonal variation brought on by yearly shifts between Ho'oilo and Kau and periodic climatic cycles, such as ENSO and PDO (Figure 5). Over the 16-month sampling period, the transect experienced two consecutive Ho'oilo through the transition between La Niña to El Niño under a high rainfall PDO epoch. Average monthly temperatures display the typical response to seasonal change, with lower temperatures

Downloaded From: https://complete.bioone.org/journals/Pacific-Science on 05 Jul 2025
Terms of Use: https://complete.bioone.org/terms-of-use

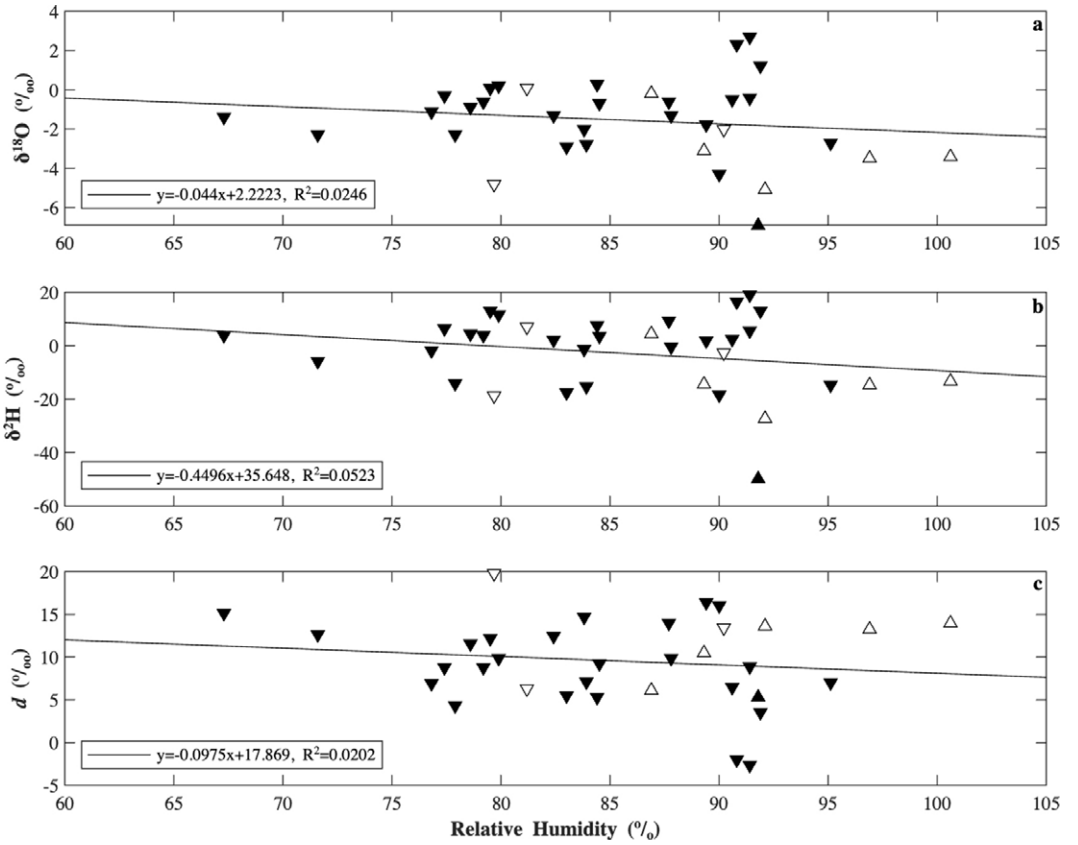

FIGURE 4. Linear regression of (*A*) $\delta^{18}O$, (*B*) $\delta^{2}H$, and (*C*) *d* values, from event-based precipitation, against corresponding relative humidity. There is no relationship between rainfall depth and any of the stable isotope variables.

during Hoʻoilo and higher temperatures during Kau. Average RH does not show any trends with seasonal variation and fluctuates regardless of Hoʻoilo and Kau. Weather conditions along the transect were generally consistent with reported archipelago-wide conditions (NOAA 2018, 2019). Along the transect, RH was lower in December and January of 2017–2018 Hoʻolio, during which archipelago-wide conditions were reported to be dry (Figure 5*A*). A decrease in RH occurred after the transition from Hoʻoilo to Kau in April 2018 (Figure 5*A*). With the beginning of the 2018–2019 Hoʻoilo, RH along the transect increased until November 2018, after which the area experienced an overall decrease in RH consistent with reported archipelago-wide conditions (Figure 5*A*) (NOAA 2019).

Seasonal variations in $\delta^{18}O$, $\delta^{2}H$, and *d* values are the result of changes in the evaporative conditions during Hoʻoilo and Kau (Figure 6). Certain months had evaporative conditions that were consistent with archipelago-wide conditions, and produced expected $\delta^{18}O$ and $\delta^{2}H$ values and rainfall depths based on those conditions. During both January 2018 and March 2019, when drought conditions were reported throughout the Hawaiian Islands (NOAA 2018, 2019), rainfall depths were low, and $\delta^{18}O$ and $\delta^{2}H$ values were the least negative (Table 3; Figures 6*A* and 6*B*). Isotopic composition and rainfall depth during these months are indicative of evaporative loss and amount effect, when low rainfall corresponds with less negative $\delta^{18}O$ and $\delta^{2}H$ values. During

Downloaded From: https://complete.bioone.org/journals/Pacific-Science on 05 Jul 2025
Terms of Use: https://complete.bioone.org/terms-of-use

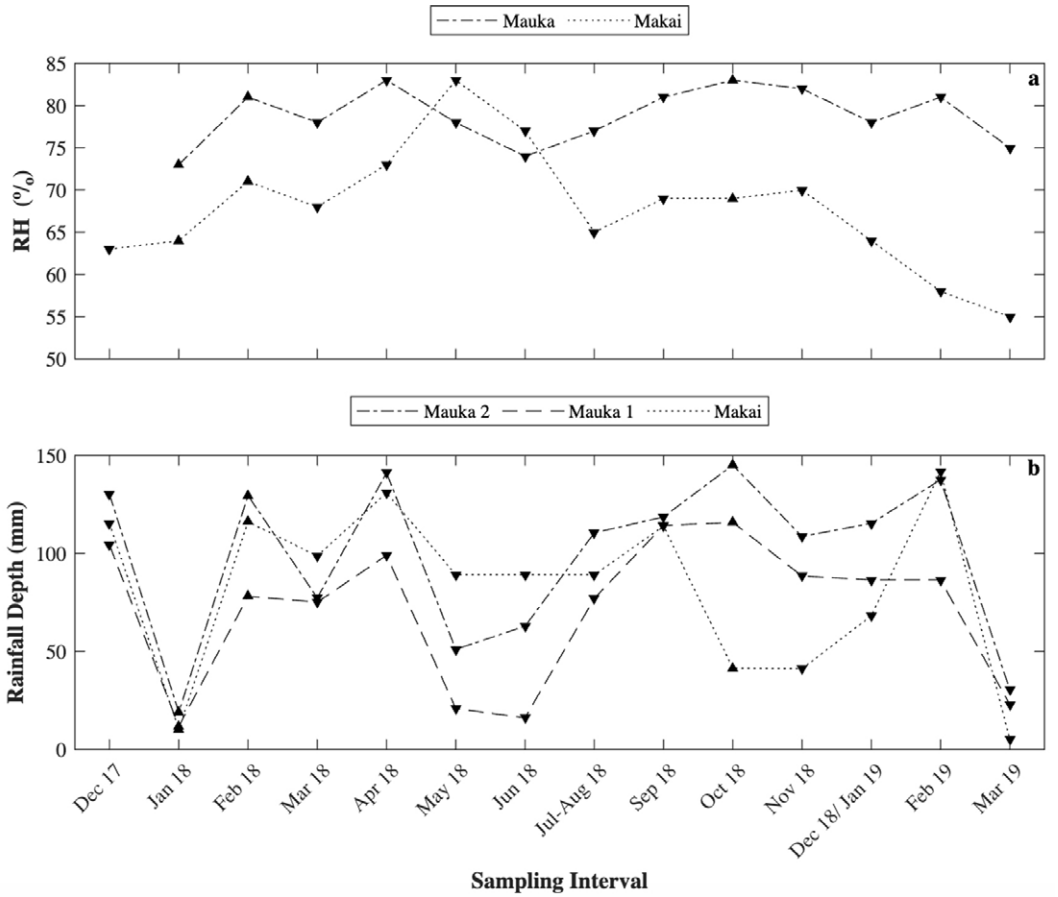

FIGURE 5. Seasonal variation of (*A*) relative humidity and (*B*) rainfall depth at each site over the sampling intervals.

February 2018, September 2018, and February 2019, when heavy rains were reported throughout the Hawaiian Islands (NOAA 2019), rainfall depth was high and $\delta^{18}O$ and $\delta^{2}H$ values were more negative (Table 3; Figures 5*B*, 6*A*, and 6*B*). Isotopic composition and rainfall depth during these months are indicative of enhanced moisture recycling and amount effect, when a greater rainfall depth corresponds with more negative $\delta^{18}O$ and $\delta^{2}H$ values.

During the months of December 2017 and November 2018, conditions along the transect were not consistent with those reported for the rest of the Hawaiian Islands (NOAA 2018, 2019). However, the relationship between isotopic composition and rainfall depth of these monthly samples was indicative of amount effect (Table 3; Figures 5*B*, 6*A*, and 6*B*). Drier conditions were reported for Hawai'i in December of the 2017–2018 Ho'oilo (NOAA 2018). Despite a lower RH, rainfall depth was high for December 2017 and $\delta^{18}O$ and $\delta^{2}H$ values were more negative (Table 3; Figures 5*B*, 6*A*, and 6*B*). Similarly, drier conditions were reported for Hawai'i in November of the 2018–2019 Ho'oilo (NOAA 2019). Along the transect, average RH was high for this month and average *T* had decreased significantly from previous consecutive months (Figure 5*A*). However, rainfall depths were relatively

Downloaded From: https://complete.bioone.org/journals/Pacific-Science on 05 Jul 2025
Terms of Use: https://complete.bioone.org/terms-of-use

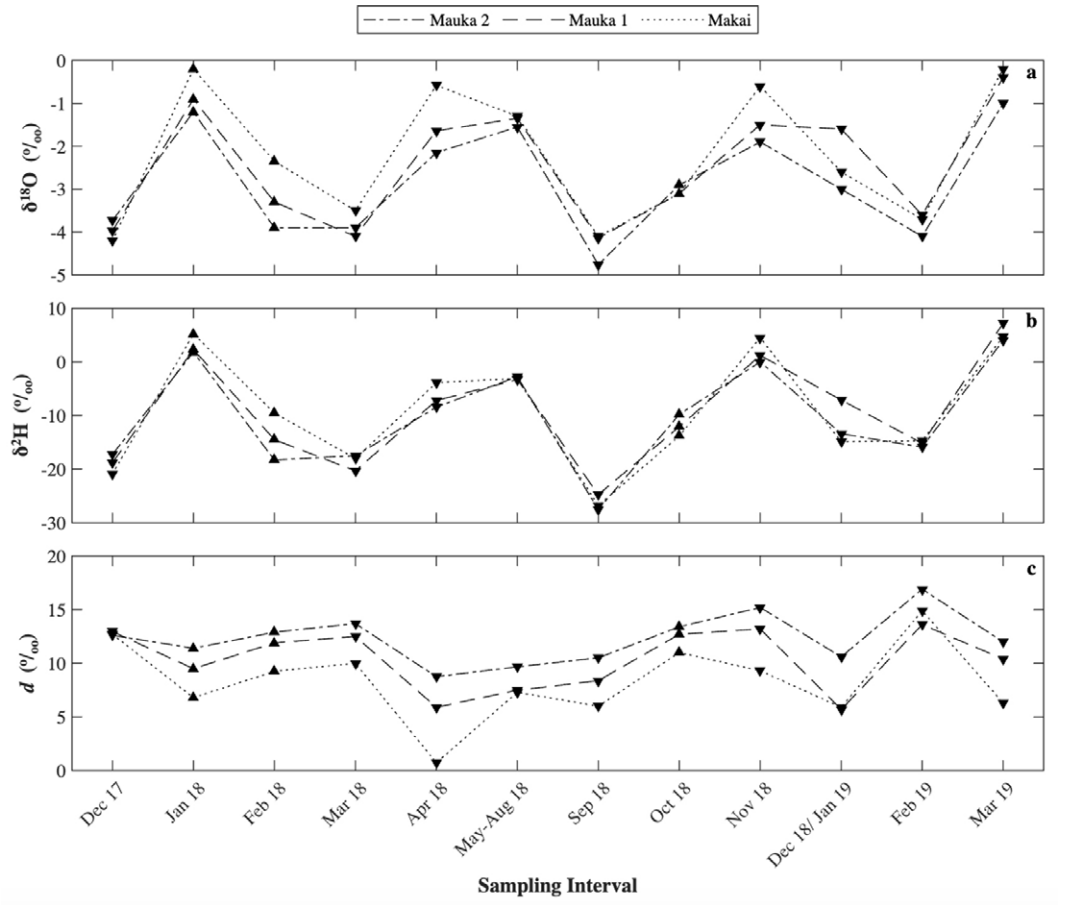

FIGURE 6. Seasonal variation of (*A*) $\delta^{18}O$, (*B*) $\delta^{2}H$, and (*C*) *d* at each site over the sampling intervals.

lower than other months, with similar evaporative conditions and $\delta^{18}O$, and $\delta^{2}H$ values less negative (Table 3; Figures 5*B*, 6*A*, and 6*B*).

Not all months of our study tied into the narrative of amount effect. Samples from the months of March 2018 and April 2018 during the transition from Hoʻoilo to Kau and October 2018 in the transition from Kau to Hoʻoilo produced such results. Heavy rain was reported for the Hawaiian Islands in March and April of the 2017–2018 Hoʻoilo. Along the transect, temperature and *d* remained constant from February to March 2018 despite a slight decrease in RH (Figures 5*A* and 6*C*). Rainfall depths from March 2018 were below average at both the Mauka 1 and Mauka 2 sites, and above average at the Makai site (Table 3). The $\delta^{18}O$ and $\delta^{2}H$ values for March 2018 were more negative, similar to months with greater rainfall depth (Figures 5*B*, 6*A*, and 6*B*). Temperature and RH increased from March to April 2018 and *d* decreased significantly (Figures 5*A* and 6*C*). Rainfall depth in April 2018 was higher than average at all collection sites, however $\delta^{18}O$ and $\delta^{2}H$ values were less negative than months with high rainfall depth (Table 3; Figures 5*B*, 6*A*, and 6*B*). With a change in season comes a change in the dominant form

Downloaded From: https://complete.bioone.org/journals/Pacific-Science on 05 Jul 2025
Terms of Use: https://complete.bioone.org/terms-of-use

of precipitation, and our collection network appears to be capturing that transition.

Results from October of the 2018–2019 Ho'oilo offer unique insights to the precipitation events that contributed to the monthly samples, as this was the first month that event-based sampling at the Makai site took place. Heavy rain was reported for Hawai'i in October 2018 (NOAA 2019). Along the transect, temperatures decreased and RH increased from September to October 2018 (Figure 5*A*). Rainfall depths were above average at both the Mauka 1 and Mauka 2 sites and below average at the Makai site (Table 3). The $\delta^{18}O$ and $\delta^{2}H$ values for this month were less negative with increased elevation. While results at the Mauka 1 and Mauka 2 sites follow the expected trends of amount effect, with greater rainfall depths corresponding to more negative $\delta^{18}O$ and $\delta^{2}H$ values, the Makai site does not. In October 2018, event-based samples were collected at the Makai site for a total of six 24 hr periods (Table 1; Figures 7 and 8). During the first four, and the very last, of these 24 hr periods, the heaviest shower accumulated 7.1 mm/min for 30 min, and the longest shower lasted for 80 min with a peak rate of 17.8 mm/min. A total of 4 mm was collected and $\delta^{18}O$ and $\delta^{2}H$ values ranged from −4.7‰

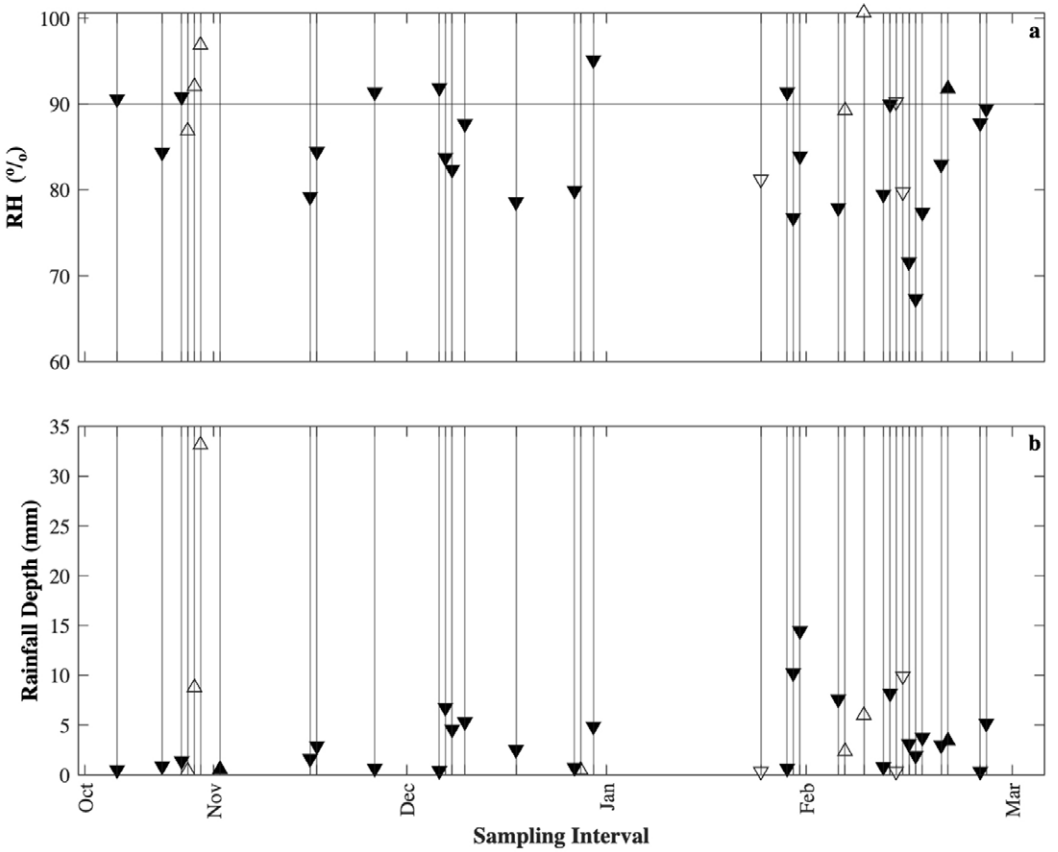

FIGURE 7. Variables: (*A*) relative humidity (RH) during precipitation and (*B*) rainfall depth for event based samples over the sampling period. "▲" and "△" indicate multiple-shower and single-shower precipitation events, respectively, coming from the South. "▼" and "▽" indicate multiple shower and single shower precipitation events, respectively, coming from the North.

Downloaded From: https://complete.bioone.org/journals/Pacific-Science on 05 Jul 2025
Terms of Use: https://complete.bioone.org/terms-of-use

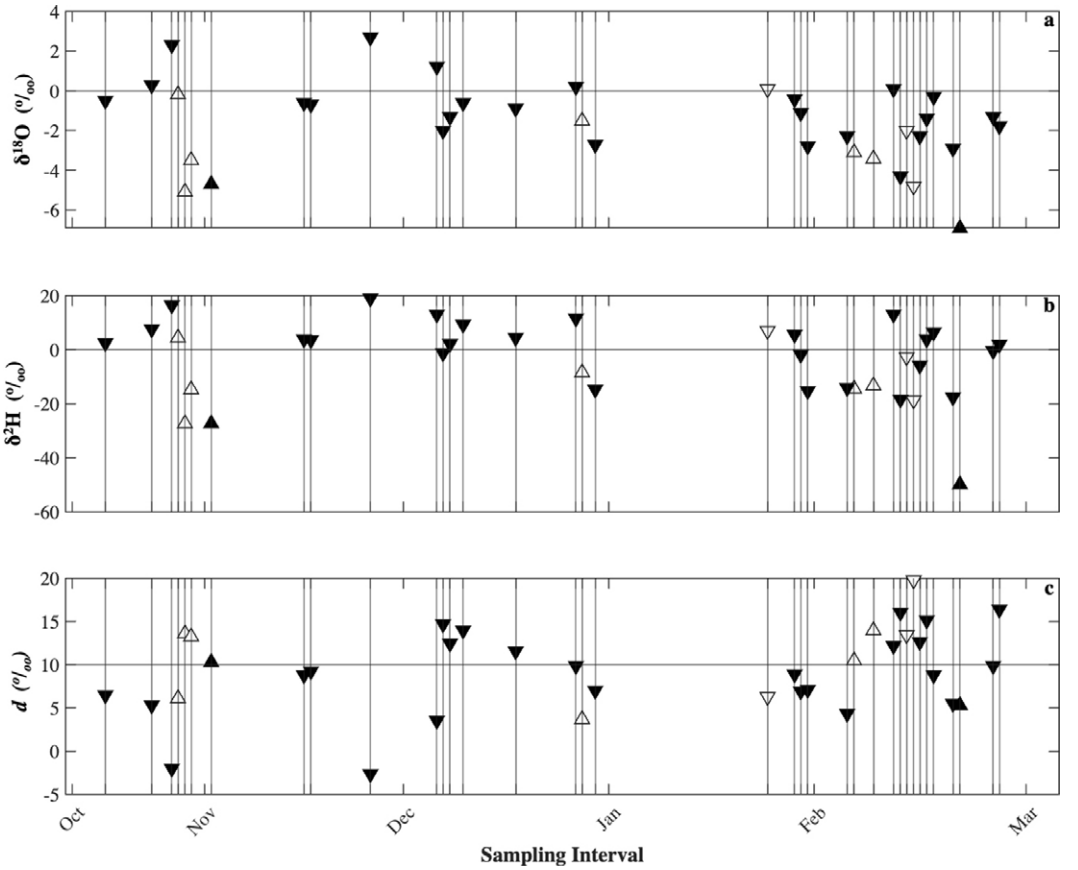

FIGURE 8. Isotopic composition: (*A*) $\delta^{18}O$, (*B*) $\delta^{2}H$, and (*C*) *d* of event based samples over the sampling period. "▲" and "△" indicate multiple-shower and single-shower precipitation events, respectively, coming from the South. "▼" and "▽" indicate multiple shower and single shower precipitation events, respectively, coming from the North.

to 2.3‰ and −27.3‰ to 16.4‰, respectively (Table 1; Figures 7*B*, 8*A*, and 8*B*). Despite the high rainfall intensity of these showers, a uniform relationship between isotopic composition and rainfall rate was not present for the Makai site.

The majority of the precipitation from October 2018 comes from a single 24 hr period on October 30, during which 57 mm was collected. The collective rainfall depth of precipitation events from 30 October 2018 is 15 mm more than the monthly sample. The $\delta^{18}O$ and $\delta^{2}H$ values from the two samples collected from this 24 hr period are more negative than most of the samples from that month (Table 1; Figures 8*A* and 8*B*). The high rainfall depth for this precipitation event corresponds to more negative $\delta^{18}O$ and $\delta^{2}H$ monthly values, demonstrating the amount effect for this sample period (Figure 7*B*).

Local Meteoric Water Line

Previous similar studies (Scholl et al. 1996, Scholl et al. 2002, Dores et al. 2020, Fackrell et al. 2020, Tachera et al. 2021) have derived the LMWL from the VWA of $\delta^{18}O$ and $\delta^{2}H$ values for the duration of the sampling period for each collection site. These other studies on Hawai'i Island, Maui, and O'ahu covered

Downloaded From: https://complete.bioone.org/journals/Pacific-Science on 05 Jul 2025
Terms of Use: https://complete.bioone.org/terms-of-use

elevation changes up to 3,500 m, while the present transect is highly localized and covers an elevation change of only 322 m. While the smaller geographic resolution and limited number of sample collection sites of this study does not allow for the creation of a standard LMWL, we can use the GMWL (Craig 1961) as a tool to evaluate the environmental variables defining our data.

The HIG-UH Mānoa sampling location of Dores et al. (2020) was located 1.5 km due north of our Makai site and 1 km due west of our Mauka 1 site (highly proximal) and collected precipitation on O‘ahu from April 2017 to July 2018, thus in partial overlap with this study. As such, this station provides a good reference for the data collected in our study. It is important to note that (1) the HIG-UH Mānoa station is located at the base of a valley whereas all three stations from this experiment are positioned along a ridgeline, and (2) the Dores et al. (2020) stations were sampled once every three months in contrast to the high resolution monthly and event-based scale described herein. While the difference in resolution between the two studies makes results difficult to interpret, the studies do appear to show strong agreement during the Ho‘oilo months of December 2017 and February–March 2018. January 2018, as well as the transition month of April 2018 and Kau months of May–July 2018, show greater variance across the two studies (Table 3). This result supports the hypothesis that large convective storm systems reaching O‘ahu—which bring large amounts of rainfall to broad geographic regions in a short period of time—have a more uniform isotopic composition in precipitation than stratiform or orographic rainfall—which travels from its original moisture source across a more localized region of the island. The large convective storms, such as Kona Lows, are more typical in the Ho‘oilo months, and appear to homogenize the precipitation chemistry during this period of analyses for both studies. The more localized stratiform or orographic precipitation typical of the Kau months has more variable isotopic compositions both (i) with each event and (ii) within each event at each specific location, as evaporative and moisture recycling conditions change. Geographically, such trade wind-based stratiform and orographic precipitation is common on the ridgelines of O‘ahu (Mink 1960, 1962), where the collectors were deployed for the duration of our study.

Where the GMWL is a standard for the relationship between $\delta^{18}O$ and $\delta^{2}H$, a slope of <8 suggests that precipitation of a region experiences faster evaporation characteristic of drier air (Dansgaard 1964). Applying this concept to a comparison of our data to the slopes of the other LMWLs from Hawai‘i, further consequences of study site resolution are observed. The sampling transect is representative of the leeward face of the Ko‘olau Range and is therefore inherently drier than the windward face of O‘ahu and the mountainous high elevations sites on Maui and Hawai‘i island (Chu et al. 2010, Giambelluca et al. 2013). The data collected in this study reflects the relatively drier climate found in leeward facing Kona districts (Figure 2).

Isotopic fractionation through moisture recycling and loss to evaporation is evident along the sampling transect as more negative $\delta^{18}O$ and $\delta^{2}H$ values lie above the GMWL and less negative $\delta^{18}O$ and $\delta^{2}H$ values lie below the GMWL (Figure 2). Furthermore, the influence of the change in RH with elevation on *d* is apparent when the monthly sample data are compared to the GWML and *d* gradient (Figure 2). Data for samples from the Mauka 2 site are typically above the GMWL and data for samples from the Makai site are typically below the GMWL. Direction of the storm does not show any influence on *d*.

The intensity and duration of precipitation over the monthly sampling intervals are evident in the comparison of monthly rainfall depths and placement along the GMWL. Samples with lower rainfall depth tend to have less negative $\delta^{18}O$ and $\delta^{2}H$ values, and samples with greater rainfall depths tend to have more negative $\delta^{18}O$ and $\delta^{2}H$ values, indicative of amount effect (Dansgaard 1964) (Figure 2). Again, elevation and seasonal variations related to storm type, including stratiform and orographic precipitation of

Downloaded From: https://complete.bioone.org/journals/Pacific-Science on 05 Jul 2025
Terms of Use: https://complete.bioone.org/terms-of-use

trade wind rainfall vs. convective precipitation of Kona storms, have observed influence on isotopic composition. Storm direction has not been identified as a useful metric in this study, although further research may provide a better understanding between moisture source, storm track, and isotopic composition of precipitation.

Influence of Elevation and Distance from Marine Moisture Source

While this study focuses on precipitation types through low-cost, low-infrastructure volumetric measurements, and storm track analysis, moisture source is still an important factor to consider. The continental effect can be easier to classify on larger land masses, but the island environment makes it challenging to identify a principal metric to describe the distance of a moisture source to a precipitation event. Typically, temperature and RH have an inverse relationship with each other over elevation gradients. As elevation increases, temperature decreases to meet the dew point temperature and create conditions that support precipitation. Both moisture recycling and loss to evaporation are subject to temperature and RH at the time of precipitation. Higher temperatures encourage evaporation, and preferentially push ^{16}O and ^{1}H of water into the vapor phase, one of the processes through which water molecules undergo isotopic fractionation (Dansgaard 1964). In this study, results suggest that elevation gradient and distance inland can control the evaporative conditions that influence precipitation towards moisture recycling or loss to evaporation, which in turn influences the $\delta^{18}O$, $\delta^{2}H$, and *d* values of precipitation at each collection site, as well as rainfall depth (Figure 9).

The conditions that support the evaporation of land-based moisture sources conducive to moisture recycling (high *T*, high RH) typically occur at the Mauka sites. Conversely, conditions that support the evaporation of falling moisture sources (high *T*, low RH) typically occur at the Makai site. The resulting $\delta^{18}O$ and $\delta^{2}H$ values show how isotopes of each element respond to the effects of conditions that support the evaporation of different moisture sources. Monthly $\delta^{18}O$ values are typically more negative with increased elevation (Figure 9*A*). Monthly $\delta^{2}H$ values are highly variable and show no particular trend along the elevation gradient (Figure 9*B*). However, the response of the ^{1}H and ^{2}H isotopes is evident in *d* values at each collection site. Where $d = 10$ represents equilibrium between evaporation of land-based moisture sources and falling moisture sources, *d* values >10 indicate moisture recycling of land-based sources and *d* values <10 indicate loss to evaporation of falling sources. At the Mauka 2 site *d* values are regularly >10 (Figure 9*C*), indicating that evaporative conditions at this elevation support moisture recycling. Outliers of this trend are observed in April 2018 and May–August 2018, during Kau when temperatures are higher. At the Makai site *d* values are regularly <10 (Figure 9*C*), indicating that evaporative conditions at this elevation support loss to evaporation. Outliers of this trend occur in December 2017, October 2018, and February 2019, during Hoʻoilo when conditions are more humid. At the Mauka 1 site, *d* values show the most variation, suggesting that evaporation at this site is sensitive to seasonal influences.

Volume-weighted averages of $\delta^{18}O$ and $\delta^{2}H$ from monthly samples at each site suggest that over time there is little difference between the isotopic composition of precipitation falling over the transect (Figures 9*A* and 9*B*). The influence of elevation on evaporative conditions that give rise to the resulting monthly $\delta^{18}O$ and $\delta^{2}H$ values are evident in the VWA *d* values, which reinforced the observation of moisture recycling of land-based sources at higher elevations and loss to evaporation of precipitate at lower elevations along the transect (Figure 9*C*). Again, the resulting VWA $\delta^{18}O$ and $\delta^{2}H$ values can be attributed to the resolution of the study site. While the relationship between isotopic composition and elevation has been studied on Maui and Hawaiʻi Island (Scholl et al. 1996, Scholl et al. 2002, Scholl et al. 2007, Fackrell et al. 2020), this work is the first to investigate this in detail on the island of Oʻahu.

Downloaded From: https://complete.bioone.org/journals/Pacific-Science on 05 Jul 2025
Terms of Use: https://complete.bioone.org/terms-of-use

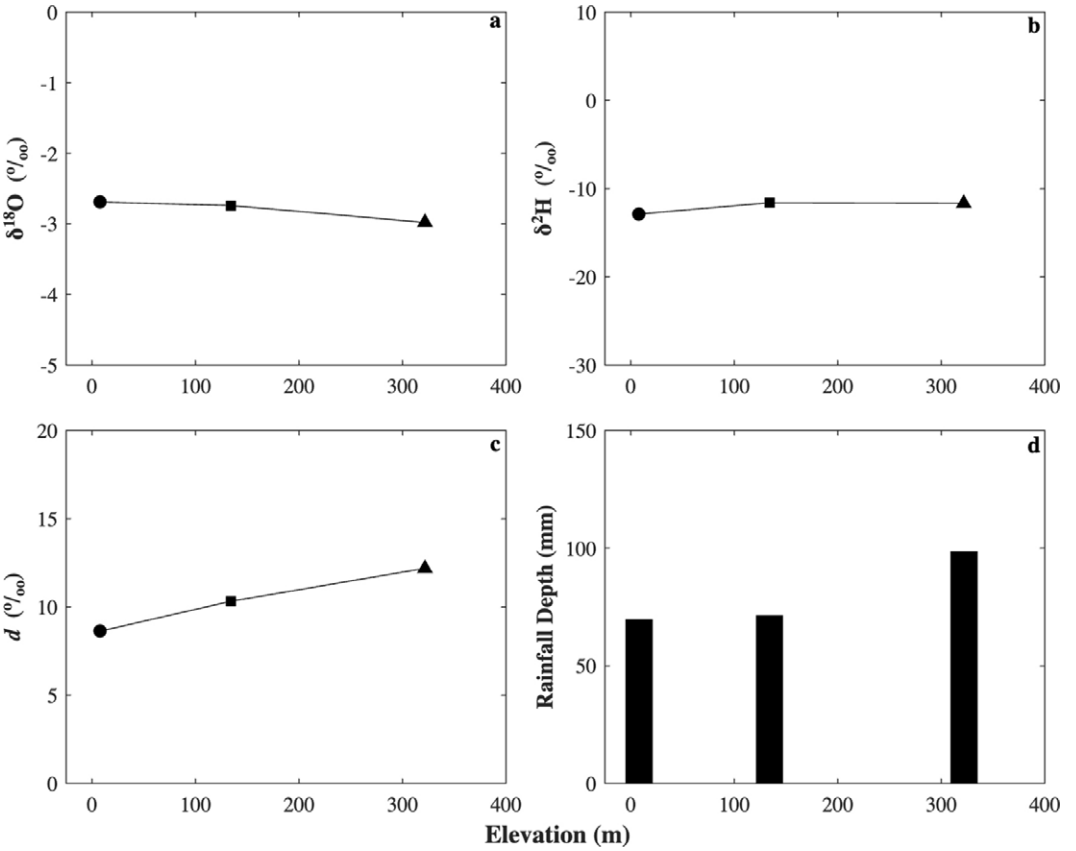

FIGURE 9. Volume-weighted average: (*A*) $\delta^{18}O$, (*B*) $\delta^{2}H$, (*C*) *d*, and (*D*) average rain depth at each site, from monthly values. In figures *A*, *B*, and *C*, "●," "■," and "▲" represent values at the Makai, Mauka 1, and Mauka 2 site, respectively.

CONCLUSION

The isotopic composition of precipitation along the sampling transect shows how elevation gradient, distance from the ocean (as a moisture source), and seasonal and climatic variations can control the evaporative conditions and give rise to the $\delta^{18}O$, $\delta^{2}H$, and *d* values of precipitation at each collection site. The VWA of $\delta^{18}O$ for the duration of the sampling period show that there is very little difference between the isotopic composition of precipitation at each. However, when the average *d* value for the duration of the sampling period is calculated, the evaporative conditions that control the isotopic composition of precipitation at each site can be explained. The low *d* value at the Makai site is indicative of loss to evaporation, while the higher *d* value at the Mauka 2 site is indicative of moisture recycling. The amount effect is another driver of the isotopic composition of precipitation along the transect. For the monthly samples, more negative $\delta^{18}O$ and $\delta^{2}H$ values were typical for greater rainfall depths. Amount effect was not observed for the event-based precipitation samples.

Event-based precipitation samples give unique insight into how individual storms and precipitation events can contribute to monthly precipitation. Examination of $\delta^{18}O$, $\delta^{2}H$, and *d*, for specific precipitation events showed atypical relationships where more negative isotopic values corresponded with low *d* values. Many of these events corresponded with both high temperature and high

Downloaded From: https://complete.bioone.org/journals/Pacific-Science on 05 Jul 2025
Terms of Use: https://complete.bioone.org/terms-of-use

RH, where the relatively higher than average temperatures caused loss to evaporation despite the high RH.

Comparison of the LMWL produced for the sampling transect with the GMWL and LMWLs from other studies in Hawai'i further suggest that enhanced moisture recycling drives the isotopic composition of precipitation at highest elevation in a transect, while loss to evaporation the driver at the lowest elevation. Differences in the slopes and *y*-intercepts can be attributed to the sample resolution and elevation gradient of the sampling transect. This study demonstrates a potential for large isotopic variability of precipitation at sites in close proximity to one another, ultimately illustrating the reality of microclimates and potential for extreme heterogeneity within Hawaiian watersheds.

FUNDING

This project has been funded by the NSF Hawai'i EPSCoR Program through the National Science Foundation's Research Infrastructure Improvement award (RII) Track-1: 'Ike Wai: Securing Hawai'i's Water Future Award # OIA-1557349. The views expressed are those of the author(s) and do not necessarily reflect the views of any of the agencies listed.

ACKNOWLEDGMENTS

The authors would like to thank CYMC Limited Partnership and Rubylyn Mata-Viti for providing access to the Makai and Mauka 2 sampling sites; Natalie Wallsgrove for assistance with sample and data analysis; and Barbara Bruno and Jennifer Engels for research support. This paper is SOEST Contribution #11362.

Literature Cited

Beven, J. L., and Wroe, D. 2019. Hurricane Lane (EP142018): National Hurricane Center, Central Pacific Hurricane Center, Tropical Cyclone Report.

Chu, P.-S., and H. Chen. 2005. Interannual and interdecadal rainfall variations in the Hawaiian Islands. J. Climate 18:4796–4813.

Chu, P.-S., Y. R. Chen, and T. A. Schroeder. 2010. Changes in precipitation extremes in the Hawaiian Islands in a warming climate. J. Climate 23:4881–4900.

Craig, H. 1961. Isotopic variations in meteoric waters. Science 133:1702–1703.

Dansgaard, W. 1964. Stable isotopes in precipitation. Tellus 4:1–33.

Diaz, H. F., T. W. Giambelluca, and J. K. Eischeid. 2011. Changes in vertical profiles of mean temperature and humidity in the Hawaiian Islands. Global Planetary Change 77:21–25.

Dores, D., C. R. Glenn, G. Torri, R. B. Whittier, and B. N. Popp. 2020. Implications for groundwater recharge from stable isotopic composition of precipitation in Hawai'i during the 2017–2018 La Niña. Hydrol. Process. 1–22.

Fackrell, J. K., C. R. Glenn, D. Thomas, R. Whittier, and B. N. Popp. 2020. Stable isotopes of precipitation and groundwater provide new insight into groundwater recharge and flow in a structurally complex hydrogeological system: West Hawai'i, USA. Hydrogeol. J. 1–17.

Froehlich, K., J. J. Gibson, and P. Aggarwal. 2002. Deuterium excess in precipitation and its climatological significance: proceedings of study of environmental change using isotope techniques. J. Geophys. Res. Atmos. 54–66.

Giambelluca, T. W., Q. Chen, A. G. Frazier, J. P. Price, Y.-L. Chen, P.-S. Chu, J. K. Eischeid, and D. M. Delparte. 2013. Online rainfall atlas of Hawai'i. Bull. Amer. Meteor. Soc. 94:313–316.

Kendall, C., and E. A. Caldwell. 1998. Isotope tracers in catchment hydrology. Pages 51–86 *in* Fundamentals in isotope geochemistry. Elsevier Science B.V. (Chapter 2).

Lee, J.-E., and I. Fung. 2006. "Amount effect" of water isotopes and quantitative analysis of post-condensation processes. Hydrol. Process. 22:1–8.

Mink, J. F. 1960. Distribution pattern of rainfall in the Leeward Koolau Mountains,

Downloaded From: https://complete.bioone.org/journals/Pacific-Science on 05 Jul 2025
Terms of Use: https://complete.bioone.org/terms-of-use

Oahu, Hawaii. J. Geophys. Res. 65 (9):2869–2876.

———. 1962. Rainfall and runoff in the Leeward Koolau Mountains, Oahu, Hawaii. Pac. Sci. 16:147–159.

Munksgaard, N. C., N. Kurita, R. Sánchez-Murillo, N. Ahmed, L. Araguas, D.L. Balachew, M. I. Bird, S. Chakraborty, N. Kien Chinh, K. M. Cobb, et al. 2019. Data descriptor: daily observations of stable isotope ratios of rainfall in the tropics. Sci. Rep. 9(1):14419. https://doi.org/10.1038/s41598-019-50973-9.

National Oceanic and Atmospheric Administration (NOAA). 2018. 2017–2018 wet season rainfall summary for Hawai'i.

———. 2019. 2018–2019 wet season rainfall summary for Hawai'i.

National Weather Service (NWS). 2018. Record Kaua'i and O'ahu rainfall and flooding – April 2018. Retrieved on June 6, 2020 from https://www.weather.gov/hfo/RecordKauaiandOahuRainfallAndFlooding-April2018.

Office of Public Health and Preparedness (OPHP). 2020. Hurricane season: State of Hawai'i. Department of Health. Retrieved on June 6, 2020 from https://health.hawaii.gov/prepare/advisories/hurricane-season/.

Pfahl, S., and H. Sodemann. 2012. What controls deuterium excess in global precipitation? Climate of the Past 10:771–781.

Putman, A. L., R. P. Fiorella, G. J. Bowen, and Z. Cai. 2019. A global perspective on local meteoric water lines: meta-analytic insight into fundamental controls and practical constraints. Water Resour. Res. 55 (8):6896–6910. https://doi.org/10.1029/2019WR025181

Scholl, M. A., S. E. Ingebritsen, C. J. Janik, and J. P. Kauahikaua. 1996. Use of precipitation and groundwater isotopes to interpret regional hydrology on a tropical volcanic island: Kilauea volcano area, Hawaii. Water Resour. Res. 32:3325–3357.

Scholl, M. A., S. B. Gingerich, and G. W. Tribble. 2002. The influence of microclimates and fog on stable isotope signatures used in interpretation of regional hydrology: East Maui, Hawaii. J. Hydrol. 264:170–184.

Scholl, M. A., T. W. Giambelluca, S. B. Gingerich, M. A. Nullet, and L. L. Loope. 2007. Cloud water in windward and leeward mountain forests: the stable isotope signature of orographic cloud water. Water Resour. Res. 43:1–13.

Scholl, M. A., J. B. Shanley, J. P. Zegarra, and T. B. Coplen. 2009. The stable isotope amount effect: new insights from NEXRAD echo tops, Luquillo Mountains, Puerto Rico. Water Resour. Res. 45(12). https://doi.org/10.1029/2008WR007515

Tachera, D. K., N. C. Lautze, G. Torri, and D. M. Thomas. 2021. Characterization of the isotopic composition and bulk ion deposition of precipitation from Central to West Hawai'i Island between 2017 and 2019. J. Hydrol. Region. Stud. 34. https://doi.org/10.1016/j.ejrh.2021.100786.

Tharammal, T., G. Bala, and D. Noone. 2017. Impact of deep convection on isotopic amount in tropical precipitation. J. Geophys. Res.: Atmos. 122:1505–1523.

Winnick, M. J., C. P. Chamberlain, J. K. Caves, and J. M. Welker. 2014. Quantifying the isotopic 'continental effect'. Earth Planet. Sci. Lett. 406:123–133.

Zwart, C., N. C. Munksgaard, A. Protat, N. Kurita, D. Lambrinidis, and M. I. Bird. 2018. The isotopic signature of monsoon conditions, cloud modes, and rainfall type. Hydrol. Process. 32(15):2296–2303. https://doi.org/10.1002/hyp.13140.

Downloaded From: https://complete.bioone.org/journals/Pacific-Science on 05 Jul 2025
Terms of Use: https://complete.bioone.org/terms-of-use